Intriguing Gold Trifluoride—Molecular Structure of Monomers and Dimers: An Electron Diffraction and Quantum Chemical Study

Balázs Réffy,† Mária Kolonits,† Axel Schulz,‡ Thomas M. Klapötke,‡ and Magdolna Hargittai*,†

Contribution from the Structural Chemistry Research Group of the Hungarian Academy of Sciences, Eötvös University, P.O. Box 32, H-1518 Budapest, Hungary, and Institute of Inorganic Chemistry, LMU—University of Munich, Butenandtstrasse 5-13 (Haus D), D-81377 Munich, Germany

Received July 26, 1999

Abstract: The molecular geometry of monomeric and dimeric gold trifluoride, AuF_3 and Au_2F_6, has been determined by gas-phase electron diffraction and high-level quantum chemical calculations. Both experiment and computation indicate that the ground-state structure of AuF_3 has C_{2v} symmetry, rather than 3-fold symmetry, with one shorter and two longer Au−F bonds and an almost T-shaped form, due to a first-order Jahn−Teller effect. CASSCF calculations show the triplet D_{3h} symmetry structure, $^3A'$, to lie about 42 kcal/mol above the $^1A_1$ symmetry ground state and the D_{3h} symmetry singlet, $^1A'$, even higher than the triplet state, by about a further 13 kcal/mol. The molecule has a typical "Mexican-hat"-type potential energy surface with three equal minimum-energy structures around the brim of the hat, separated by equal-height transition structures, about 3.6 kcal/mol above the minimum energy. The geometry of the transition structure has also been calculated. The dimer has a D_{2h} symmetry planar, halogen-bridged geometry, with the gold atom having an approximately square-planar coordination, typical for d^8 transition metals. The geometries of AuF and Au_2F_2 have also been calculated. The very short Au···Au separation in Au_2F_2 is indicative of the so-called aurophilic interaction. This effect is much less pronounced in Au_2F_6.

Introduction

Determination of precise and accurate structural parameters for a molecule containing gold is a formidable task, both for experiment and for computation. Several neutral and anionic fluorides of gold have been investigated in the past decade by ab initio techniques.[1] Density functional methods have also been applied for gold systems and proved successful even for large gold complexes.[2] The importance of including relativistic effects in the calculations has been demonstrated.[1,3] Schwerdtfeger, Dolg, and co-workers[1c] predicted AuF to be a stable gas-phase compound, based on computation, which was later confirmed in a neutralization−reionization mass spectrometric experiment by Schwarz, Klapötke, and co-workers.[4] Recently, a UV−vis spectroscopic study on gold(III) and gold(V) fluorides and fluoroanions has been published.[5]

Gold trifluoride and gold pentafluoride can only be prepared from the elements (or ClF_3 instead of F_2) and are very moisture sensitive and strong oxidizers.[6] Gold trifluoride has a rather low volatility, but heating the sample risks decomposition, so the experimental conditions have to be selected very carefully for a gas-phase investigation. The interpretation of electron diffraction data is hindered by the large atomic scattering of gold as compared to the molecular contribution, by the strong electron scattering of gold as compared with that of fluorine, by the dynamical (multiple) atom−atom scattering, and by the anharmonicity of the vibrations.

The crystal structure of gold trifluoride is unique, with square-planar AuF_4 units joined by symmetrical μ-fluoro bridges in cis positions, thus forming a helical chain.[7] The structure of its vaporization products has not yet been determined by experiment. A recent quantum chemical calculation at the Hartree−Fock (HF) level indicated that monomeric gold trifluoride is a Jahn−Teller distorted molecule with C_{2v} symmetry.[1a] As early as 1976, a simple Hückel-type calculation by Hoffmann et al. suggested a T-shaped ground-state geometry for another Au(III) molecule, $Au(CH_3)_3$, rather than one with C_{3h} symmetry, due to Jahn−Teller distortion.[8]

* To whom correspondence should be addressed. E-mail: hargittaim@ludens.elte.hu.

† Eötvös University.

‡ University of Munich.

(1) (a) Schwerdtfeger, P.; Boyd, P. D. W.; Brienne, S.; Burrell, A. K. *Inorg. Chem.* **1992**, *31*, 3411. (b) Schwerdtfeger, P.; McFeaters, J. S.; Liddell, M. J.; Hrusak, J.; Schwarz, H. *J. Chem. Phys.* **1995**, *103*, 245. (c) Schwerdtfeger, P.; McFeaters, J. S.; Stephens, R. L.; Liddell, M. J.; Dolg, M.; Hess, B. A. *Chem. Phys. Lett.* **1994**, *218*, 362. (d) Schwerdtfeger, P.; Dolg, M.; Schwarz, W. H. E.; Bowmaker, G. A.; Boyd, P. D. W. *J. Chem. Phys.* **1989**, *91*, 1762. (e) Laerdahl, J. K.; Saue, T.; Faegri, K. *Theor. Chem. Acc.* **1997**, *97*, 177.

(2) (a) Chung, S.-C.; Krueger, S.; Schmidbaur, H.; Roesch, N. *Inorg. Chem.* **1996**, *35*, 5387. (b) Hrusak, J.; Hertwig, R. H.; Schröder, D.; Schwerdtfeger, P.; Koch, W.; Schwarz, H. *Organometallics* **1995**, *14*, 1284. (c) Hrusak, J.; Hertwig, R. H.; Schröder, D.; Koch, W.; Schwarz, H. *Chem. Phys. Lett.* **1995**, *236*, 194.

(3) Pyykkö, P. *Chem. Rev.* **1988**, *88*, 563.

(4) Schroeder, D.; Hrusak, J.; Tornieporth-Oetting, I. C.; Klapötke, T. M.; Schwarz, H. *Angew. Chem.* **1994**, *106*, 223.

(5) Hector, A. L.; Levason W.; Weller, M. T.; Hope, E. G. J. *J. Fluorine Chem.* **1997**, *86*, 105.

(6) (a) Tornieporth-Oetting, I. C.; Klapötke, T. M. *Chem. Ber.* **1995**, *128*, 957. (b) Sharp, A. G. *J. Chem. Soc.* **1959**, 2901. (c) *Gmelin, Handbuch der Anorganischen Chemie, Au*; Verlag Chemie, Weinheim, 1954; p 684. (d) *Gmelin Handbook, Au Suppl. Vol. B 1*; Springer, Berlin, 1992; p 117. (e) Puddepath, R. J. *The Chemistry of Gold*; Elsevier: Amsterdam, 1978. (f) Engelmann, U.; Müller, B. G. *Z. Anorg. Allg. Chem.* **1993**, *619*, 1661. (g) Engelmann, U.; Müller, B. G. *Z. Anorg. Allg. Chem.* **1992**, *618*, 43.

(7) (a) Einstein, F. W. B.; Rao, P. R.; Trotter, J.; Bartlett, N. *J. Chem. Soc. (A)* **1967**, 478. (b) Zemva, B.; Lutar, K.; Jeshi, A.; Casteel, W. J.; Wilkonson, A. P.; Cox, D. E.; Von Dreele, R. B.; Bormann, H.; Bartlett, N. *J. Am. Chem. Soc.* **1991**, *113*, 4192.

(8) Komiya, S.; Albright, T. A.; Hoffmann, R.; Kochi, J. K. *J. Am. Chem. Soc.* **1976**, *98*, 7255.

10.1021/ja992638k CCC: $19.00
Published on Web 03/18/2000

Table 1. Experimental Conditions

	$AuF_3 + Au_2F_6$		Au_2F_6	
nozzle temperature (K)	1094		600	
accelerating voltage (kV)	60		60	
camera ranges (cm)	50	19	50	19
no. of plates[a] analyzed	4	5	4	4
data intervals ($Å^{-1}$)	2.00−14.00	9.00−29.50	2.00−14.00	9.00−29.50
data steps ($Å^{-1}$)	0.125	0.25	0.125	0.25

[a] Kodak electron image plates.

Considering the severe computational difficulties associated with such a system, a comparison with experiment seemed worthwhile. We were also curious whether the Jahn−Teller distortion could be observed experimentally, especially since such a distortion was detected recently for a similar gas-phase molecule, MnF_3, by gas electron diffraction.[9]

Experimental Section

The sample of gold trifluoride was prepared according to a method described elsewhere.[6,10] The compound is extremely sensitive to air and humidity and was handled with special care during the electron diffraction experiment. Our first attempts at registering electron diffraction patterns failed due to decomposition of the sample during heating. The photographic plates showed changing diffraction patterns, an obvious indication of decomposition of the sample. Eventually, passivation of all parts of the nozzle system that may come in contact with the gold trifluoride sample stabilized the experimental conditions. This passivation was done with fluorine gas for 24 h at 4 atm and 100 °C.

A previous mass spectrometric study[11] of gold trifluoride indicated three different species in the vapor phase. At lower temperatures dimeric molecules, while at higher temperatures monomeric molecules were registered. At low temperatures there was also an indication of the presence of a very small amount of trimeric species, which, however, proved to make no appreciable contribution to the electron diffraction analysis.

To determine the structure of both monomeric and dimeric forms of gold trifluoride, two independent experiments were performed. One was done at the lowest temperature that provided sufficient vapor pressure to have the largest relative abundance of dimers in the vapor. The other, higher-temperature experiment, aimed at detecting the monomer molecules, had to be planned especially carefully for the reasons mentioned above.

The electron diffraction patterns were recorded in the modified EG-100A apparatus of the Budapest laboratory.[12] A high-temperature nozzle system was used at 600 K[13] and a double-oven system at 1094 K.[14] The nozzle material was nickel. In the higher-temperature experiment the evaporating molecules, reaching the cold surfaces of the apparatus, decomposed to gold metal and either fluorine gas or hydrogen fluoride (by reacting with residual water in the apparatus). After the experiment a thin gold layer covered the walls of the apparatus and even the photographic plates. This was carefully removed mechanically with a piece of cotton swab after the plates were developed. The increased experimental uncertainties, especially those of the vibrational amplitudes, show the consequences of these experimental difficulties. The presence of any appreciable amount of HF and F_2 in the scattering volume was checked and could be ruled out in the structure analysis.

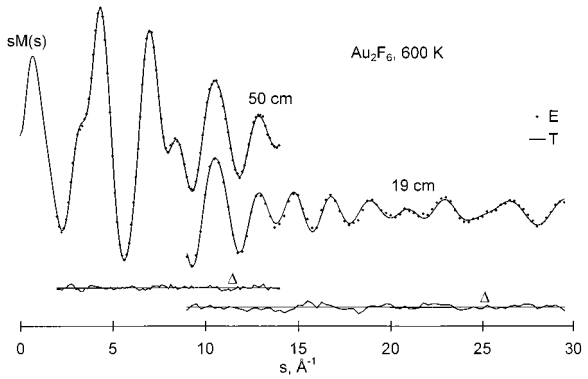

Figure 1. Experimental (E) and calculated (T) molecular intensities and their differences (Δ); electron diffraction at 600 K.

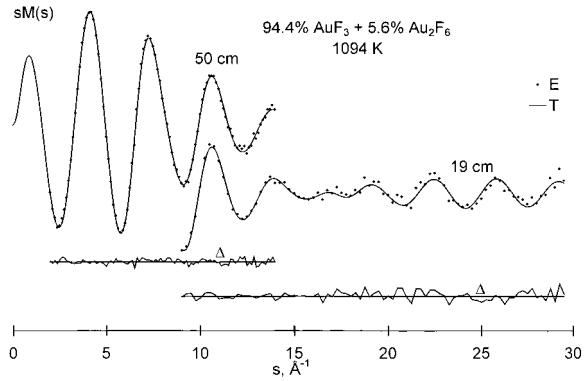

Figure 2. Experimental (E) and calculated (T) molecular intensities and their differences (Δ); electron diffraction at 1094 K.

Details of the experiments are given in Table 1. The electron scattering factors were taken from the literature.[15] The experimental and calculated molecular intensities from the two experiments are shown in Figures 1 and 2.

Computational Details

Different electronic states and geometries had to be checked for monomeric AuF_3 because of the possible Jahn−Teller distortion (vide supra). Single reference calculations do not suffice for reliable comparison of different triplet and singlet states; therefore, as a first step, different geometrical arrangements were checked with a CASSCF calculation. We correlated four electrons in six orbitals, to give 105 CSF. Pseudopotential techniques were adopted for Au (see below), and a 6-31G(d) standard basis set was applied for fluorine. Four different planar states were investigated, two with C_{2v} ($^1A_1$) and two with D_{3h} symmetry ($^3A'$, $^1A'$). The two C_{2v} symmetry states represent the ground state and a transition state, separated by 3.6 kcal/mol. The triplet state is 41.7 kcal/mol higher in energy than the ground state, followed by the open-shell biradical singlet state with a further 13.4 kcal/mol higher energy, all at the CASSCF level.

These and some of the geometry optimizations have been performed using the GAUSSIAN94 program package,[16] while the latest ones were

(9) Hargittai, M.; Réffy, B.; Kolonits, M.; Marsden, C.; Heully, J.-L. *J. Am. Chem. Soc.* **1997**, *119*, 9042.

(10) Klapötke, T. M. In *Organic Derivatives of Silver and Gold*; Patai, S., Ed.; J. Wiley: Chichester, Sussex, 1999; Chapter 15 and refs 155−169 therein.

(11) Chilingarov, N. S.; Korobov, M. V.; Rudometkin, S. V.; Alikhanyan, A. S.; Sidorov, L. N. *Int. J. Mass Spectrom. Ion Processes* **1986**, *69*, 175.

(12) Hargittai, I.; Tremmel, J.; Kolonits, M. *HSI Hung. Sci. Instrum.* **1980**, *50*, 31.

(13) Tremmel, J.; Hargittai, I. *J. Phys. E Sci. Instrum.* **1985**, *18*, 148.

(14) Hargittai, M.; Kolonits, M.; Gödörházy, L. *Chem. Phys. Lett.* **1996**, *257*, 321.

(15) Ross, A. W.; Fink, M.; Hilderbrandt, R.; Wang, J.; Smith, V. H., Jr. In *International Tables for Crystallography*, *C*; Wilson, A. J. C., Ed.; Kluwer: Dordrecht, 1995; pp 245−338.

Table 2. Geometrical Parameters and Total Energies of Gold Fluoride Molecules: AuF_3 in Different Electronic States, Au_2F_6, AuF, and Au_2F_2, from Computation[a]

level	B3LYP	B3LYP	B3LYP	B3LYP	B3LYP	MP2	B3LYP	MP2
basis for Au	basis 1	basis 1	basis 1	basis 1	basis 2	basis 2	basis 2	basis 2
basis for F	6-311+G(3d)	6-311+G(3df)	aug-cc-PVDZ	aug-cc-PVTZ	6-311+G(3df)	6-311+G(3df)	aug-cc-PVTZ	aug-cc-PVTZ
				AuF_3, $^1A_1$, GS[b]				
Au_1-F_2	1.916	1.914	1.927	1.905	1.902	1.873	1.890	1.846
Au_1-F_3	1.926	1.924	1.934	1.919	1.919	1.903	1.910	1.881
$\Delta(Au_1-F_3-Au_1-F_2)$	0.010	0.010	0.007	0.014	0.017	0.030	0.020	0.035
$\angle F_2-Au_1-F_3$	94.7	94.6	94.6	94.4	94.3	92.9	94.3	92.8
total energy	−435.299117	−435.301189	−435.1998692	−435.3154317	−435.444875	−434.518371	−435.4602479	−434.565278
				AuF_3, $^1A_1$, TS[c]				
Au_1-F_2	1.932	1.930	1.930	1.925	1.926	1.903	1.915	1.880
Au_1-F_3	1.916	1.913	1.914	1.907	1.904	1.886	1.895	1.861
$\angle F_2-Au_1-F_3$	139.3	139.4	139.4	139.4	139.1	140.3	139.3	140.2
total energy	−435.290602	−435.292647	−435.2244649	−435.3068579	−435.433895	−434.505749	−435.4499905	−434.5532185
				AuF_3, $^3A'$ D_{3h}				
Au−F	1.959	1.957	1.957					
total energy	−435.280435	−435.281983	−435.2138657					
				Au_2F_6, D_{2h}[d]				
$Au-F_t$	1.904	1.901	1.912	1.895	1.893	1.873	1.882	1.850
$Au-F_b$	2.063	2.061	2.081	2.059	2.057	2.030	2.052	2.016
$\Delta(Au-F_b-Au-F_t)$	0.159	0.160	0.169	0.164	0.164	0.157	0.169	0.166
Au···Au	3.194	3.191	3.237	3.186	3.183	3.075	3.168	3.073
$\angle F_t-Au-F_t$	89.9	89.9	89.5	89.7	89.7	89.4	89.7	89.1
$\angle F_b-Au-F_b$	78.5	78.5	77.9	78.6	78.6	81.5	78.9	80.7
total energy	−870.700372	−870.704426	−870.5073501	−870.7316871	−870.99478	−869.164075	−871.0233096	−869.254089
				AuF				
Au−F	1.981	1.979	1.976	1.973	1.977	1.944	1.965	1.911
total energy	−235.617198	−235.617648	−235.5834667	−235.6221034	−235.762839	−235.139821	−235.767479	−235.1544586
				Au_2F_2				
Au−F	2.260	2.258	2.260	2.261	2.261	2.215	2.264	2.215
Au···Au	2.877	2.876	2.890	2.856	2.851	2.711	2.834	2.709
∠F−Au−F	100.9	100.9	100.5	101.7	101.8	104.5	102.4	104.6
total energy	−471.258046	−471.258313	−471.1950437	−471.2649946	−471.549200	−470.327308	−471.5559185	−470.3523033

[a] Distances in angstroms, angles in degrees, total energies in hartrees. For numbering of atoms, see Figure 3. [b] Ground state. [c] Transition state. [d] $Au-F_t$ and $Au-F_b$ denotes terminal and bridging bonds of the dimer, respectively.

performed with GAUSSIAN98.[17] For gold, two slightly different sets of pseudopotentials and basis sets were used. First, the multielectron adjusted quasirelativistic effective core potential (WB-MEFIT), covering 60 electrons ($[Kr]4d^{10}4f^{14}$) and an (8s7p6d)/[6s5p3d]-GTO valence basis set (311111,22111,411), of the Stuttgart group was used (hereafter referred to as basis 1).[18] The use of this pseudopotential makes the treatment of major relativistic effects—Darwin and mass velocity terms—feasible. Spin−orbit interaction is not included. Full electron basis sets were utilized for fluorine, ranging from 6-31G(d) to 6-311+G(3df), along with the Dunning correlation-consistent basis sets, aug-cc-pVDZ and aug-cc-pVTZ.[19] At the final stage of the computations an optimized pseudopotential and a larger basis set were used for gold,[20] with additional d and f polarization functions (2111111111,41111,-211111,1111) (hereafter referred to as basis 2) and two different standard basis sets for fluorine, 6-311+G(3df) and aug-cc-pVTZ.

Full geometry optimizations were performed for the ground- and excited-state AuF_3 molecules, using a Fletcher−Powell procedure, at two different levels of theory, MP2 and density functional (B3LYP).[21,22] The D_{3h} symmetry structure was calculated only at lower computational levels. All stationary points were characterized by a frequency analysis at the B3LYP level and using basis 1 for gold and the 6-311+G(3d) basis set for fluorine.

The potential energy surface (PES) of AuF_3 was calculated using the aug-cc-pVDZ basis set for fluorine and the Stuttgart pseudopotential and basis 1 for gold. The energy was calculated as a function of the two F−Au−F angles in 5° steps. None of the determined points has been corrected for zero-point vibrations; such corrections are calculated to be very small, of the order of 0.1−0.2 kcal/mol, in the harmonic approximation.

Dimeric gold trifluoride has also been calculated at all levels of theory applied for the monomer. To take into account the possibility of AuF_3 being reduced to AuF or Au_2F_2, the geometries of these two species were also calculated at all computational levels used for gold trifluoride. The geometrical parameters are presented in Table 2. The relative energies and dimerization energies are shown in Table 3. Both dimerizations are exothermic, but the energy gain in the dimerization of AuF_3 is much larger, by about 50 kcal/mol, than that for AuF. The

(16) Frisch, M. J.; Trucks, G. W.; Schlegel, H. B.; Gill, P. M. W.; Johnson, B. G.; Robb, M. A.; Cheeseman, J. R.; Keith, T.; Petersson, G. A.; Montgomery, J. A.; Raghavachari, K.; Al-Laham, M. A.; Zakrzewski, V. G.; Ortiz, J. V.; Foresman, J. B.; Cioslowski, J.; Stefanov, B. B.; Nanayakkara, A.; Challacombe, M.; Peng, C. Y.; Ayala, P. Y.; Chen, W.; Wong, M. W.; Andres, J. L.; Replogle, E. S.; Gomperts, R.; Martin, R. L.; Fox, D. J.; Binkley, J. S.; Defrees, D. J.; Baker, J.; Stewart, J. P.; Head-Gordon, M.; Gonzalez, C.; Pople, J. A. *Gaussian 94*, Revision E.2; Gaussian, Inc.: Pittsburgh, PA, 1995.

(17) Frisch, M. J.; Trucks, G. W.; Schlegel, H. B.; Scuseria, G. E.; Robb, M. A.; Cheeseman, J. R.; Zakrzewski, V. G.; Montgomery, J. A., Jr.; Stratmann, R. E.; Burant, J. C.; Dapprich, S.; Millam, J. M.; Daniels, A. D.; Kudin, K. N.; Strain, M. C.; Farkas, O.; Tomasi, J.; Barone, V.; Cossi, M.; Cammi, R.; Mennucci, B.; Pomelli, C.; Adamo, C.; Clifford, S.; Ochterski, J.; Petersson, G. A.; Ayala, P. Y.; Cui, Q.; Morokuma, K.; Malick, D. K.; Rabuck, A. D.; Raghavachari, K.; Foresman, J. B.; Cioslowski, J.; Ortiz, J. V.; Stefanov, B. B.; Liu, G.; Liashenko, A.; Piskorz, P.; Komaromi, I.; Gomperts, R.; Martin, R. L.; Fox, D. J.; Keith, T.; Al-Laham, M. A.; Peng, C. Y.; Nanayakkara, A.; Gonzalez, C.; Challacombe, M.; Gill, P. M. W.; Johnson, B.; Chen, W.; Wong, M. W.; Andres, J. L.; Gonzalez, C.; Head-Gordon, M.; Replogle, E. S.; Pople, J. A. *Gaussian 98*, Revision A.6; Gaussian, Inc.: Pittsburgh PA, 1998.

(18) Andrae, D.; Häussermann, U.; Dolg, M.; Stoll, H.; Preuss, H. *Theor. Chim. Acta* **1990**, *77*, 123.

(19) (a) Woon, D. E.; Dunning, T. H. *J. Chem. Phys.* **1993**, *98*, 1358. (b) Kendall, R. A.; Dunning, T. H.; Harrison, R. J. *J. Chem. Phys.* **1992**, *96*, 6796. (c) Dunning, T. H. *J. Chem. Phys.* **1989**, *90*, 1007.

(20) Dolg, M., private communication.

(21) Becke, A. D. *J. Chem. Phys.* **1993**, *98*, 5648.

(22) (a) Lee, C.; Yang, W.; Parr, R. G. *Phys. Rev. B* **1988**, *37*, 785. (b) Miehlich, B.; Savin, A.; Stoll, H.; Preuss, H. *Chem. Phys. Lett.* **1989**, *157*, 200.

Table 3. Relative Energies and Dimerization Energies (kcal/mol)

level	B3LYP	B3LYP	B3LYP	B3LYP	B3LYP	MP2	B3LYP	MP2
basis for Au	basis 1	basis 1	basis 1	basis 1	basis 2	basis 2	basis 2	basis 2
basis for F	6-311+G(3d)	6-311+G(3df)	aug-cc-PVDZ	aug-cc-PVTZ	6-311+G(3df)	6-311+G(3df)	aug-cc-PVTZ	aug-cc-PVTZ
				AuF_3, TS−GS				
ΔE, 0 K	5.3	5.4	5.2	5.4	6.9	7.9	6.3	7.6
$\Delta_R H$, 298 K	4.7	4.8	4.6	4.8	6.3	7.3	5.7	7.0
				$2AuF \rightarrow Au_2F_2$				
ΔE, 0 K	−14.8	−14.4	−17.6	−13.0	−14.8	−29.9	−13.2	−27.2
$\Delta_R H$, 298 K	−14.5	−14.1	−18.1	−13.5	−14.5	−29.6	−13.7	−27.7
				$2AuF_3 \rightarrow Au_2F_6$				
ΔE, 0 K	−64.1	−64.0	−67.6	−63.3	−65.9	−79.9	−64.5	−77.5
$\Delta_R H$, 298 K	−62.5	−62.5	−67.3	−63.0	−64.4	−78.4	−63.0	−76.1

Table 4. Vibrational Frequencies, Symmetry Assignments, and Infrared Intensities for the Ground-State Molecules of AuF_3, Au_2F_6, AuF, and Au_2F_2 from B3LYP Computations[a]

AuF_3	Au_2F_6	AuF	Au_2F_2
B_2 131 (2)	B_{3u} 72 (3)	σ 513 (41)	B_{3g} 39 (0)
B_1 191 (13)	A_g 121 (0)		A_g 55 (0)
A_1 206 (10)	B_{2u} 125 (1)		B_{3u} 62 (17)
A_1 593 (18)	A_u 129 (0)		B_{1u} 222 (118)
A_1 604 (0)	B_{3g} 172 (0)		B_{2u} 292 (71)
B_2 640 (140)	B_{2g} 172 (0)		A_g 347 (0)
	B_{1g} 200 (0)		
	B_{1u} 217 (2)		
	A_g 230 (0)		
	B_{3u} 230 (16)		
	B_{3g} 416 (0)		
	B_{2u} 471 (14)		
	B_{1u} 471 (250)		
	A_g 486 (0)		
	B_{3g} 626 (0)		
	B_{2u} 636 (93)		
	B_{1u} 636 (127)		
	A_g 644 (0)		

[a] Frequencies in cm^{-1}, IR intensities (in parentheses) in km/mol. Applied basis sets: F, 6-311+G(3d); Au, basis 1. ZPE (in kcal/mol) for AuF_3, 3.381; for Au_2F_6, 8.654; for AuF, 0.733; for Au_2F_2, 1.453.

calculated BSSE lies in the range of 1 kcal/mol (B3LYP, Au, basis 1; F, 6-311+G(3df)). Vibrational frequencies for the ground-state molecules are given in Table 4. The models of all molecules and the numbering of atoms are given in Figure 3.

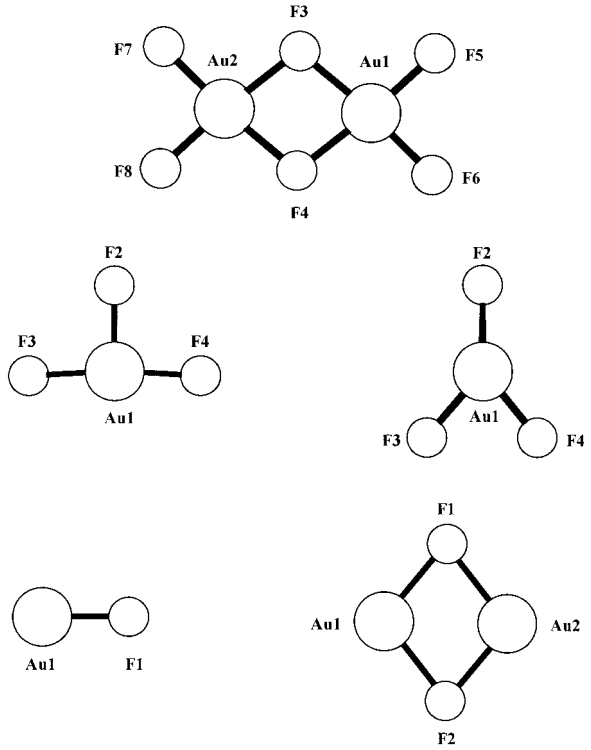

Figure 3. Models of gold fluoride molecules and the numbering of atoms.

Normal Coordinate Analysis

Normal coordinate analyses were carried out for AuF_3 and Au_2F_6 based on the computed frequencies and force fields (vide supra). Two programs were used, both based on the harmonic approximation, ASYM20[23] using rectilinear displacements and SHRINK4[24] using curvilinear displacements. Table 5 lists the computed mean-square amplitudes from both approaches together with the experimental values. The two approaches give the same results for parallel amplitudes and are in agreement with the available experimental values within their uncertainties.

Electron Diffraction Analysis

Lower-Temperature Experiment. The electron diffraction experiment at 600 K was analyzed first. It corresponds to scattering by the dimeric gold trifluoride molecule alone. The presence of other species, such as the monomer and trimer molecules, fluorine, or hydrogen fluoride, were tested and ruled out.

For fluxional systems modern electron diffraction analyses are carried out either with the so-called dynamical analysis or in the so-called r_α representation, both in order to avoid the effects of large-amplitude deformation vibrations on the determined parameters. The correctness of the latter approach has recently been questioned.[24] Moreover, for such strongly anharmonic systems as the high-temperature metal halides, the value of purely harmonic vibrational corrections is questionable. Nonetheless, we performed refinements with both the rectilinear and the curvilinear vibrational corrections, but the agreement with experiment was worse than that from the conventional analysis in both cases. Moreover, the refinements were unstable; therefore, we decided not to adopt either approach. An anharmonic vibrational analysis or the quantum chemical calculation of anharmonicity parameters is not yet feasible for such molecules. On the other hand, in a conventional so-called static electron diffraction analysis the shrinkage effect[25] is not compensated for, and this hinders the determination of the symmetry of the equilibrium geometry. In our study, a lower,

(23) Hedberg, L.; Mills, I. M. *J. Mol. Spectrosc.* **1993**, *160*, 117.

(24) Sipachev, V. A. In *Advances in Molecular Structure Research*; Hargittai, M., Hargittai, I. Eds.; JAI Press: Stamford, CT, 1999; Vol. 5, pp 263−311.

(25) See, e.g.: Kuchitsu, K. In *Diffraction Studies on Non-Crystalline Substances*; Hargittai, I., Orville-Thomas, W. J., Eds.; Elsevier: Amsterdam, 1981; pp 63−116.

Table 5. Mean-Square Amplitudes of Vibration for Au_2F_6 and AuF_3 from Different Normal Coordinate Analyses and from Experiment

	Au_2F_6						AuF_3			
	600 K			1094 K				1094 K		
	l_{ASYM20}	$l_{SHRINK4}$	l_{exp}	l_{ASYM20}	$l_{SHRINK4}$	l_{exp}		l_{ASYM}	$l_{SHRINK4}$	l_{exp}
Au_1-F_5	0.049	0.050	0.049 ± 0.004	0.063	0.063	0.059 ± 0.006[a]	Au_1-F_2	0.067	0.067	0.063 ± 0.006[c]
Au_1-F_3	0.069	0.069	0.067 ± 0.004	0.090	0.090	0.086 ± 0.006[a]	Au_1-F_3	0.064	0.066	0.060 ± 0.006[c]
$Au_1\cdots Au_2$	0.084	0.085	0.095 ± 0.003	0.113	0.116	0.111 ± 0.038	$F_2\cdots F_3$	0.250	0.262	0.242 ± 0.061
$Au_1\cdots F_7$	0.128	0.127	0.140 ± 0.007	0.172	0.173	0.197 ± 0.118	$F_3\cdots F_4$	0.105	0.092	0.105[b]
$F_3\cdots F_4$	0.097	0.100	0.097[b]	0.127	0.132	0.127[b]				
$F_3\cdots F_5$	0.152	0.150	0.171 ± 0.023	0.203	0.201	0.203[b]				
$F_5\cdots F_6$	0.140	0.141	0.159 ± 0.023	0.186	0.189	0.186[b]				
$F_3\cdots F_6$	0.083	0.083	0.086 ± 0.009	0.108	0.109	0.108[b]				
$F_5\cdots F_7$	0.215	0.212	0.296 ± 0.111	0.289	0.292	0.289[b]				
$F_5\cdots F_8$	0.136	0.133	0.177 ± 0.057	0.181	0.186	0.181[b]				

[a] Refined in a group with the amplitudes of the monomer Au−F bond lengths. [b] Value taken from the normal coordinate analysis. [c] Refined in a group with the amplitudes of the dimer Au−F bond lengths.

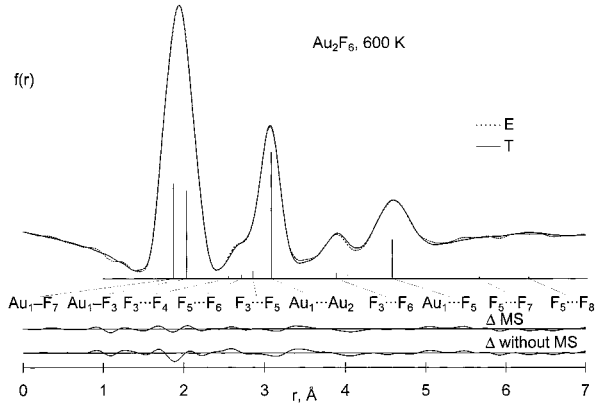

Figure 4. Experimental (E) and calculated (T) radial distributions; experiment at 600 K. The difference curves "ΔMS" and "Δ without MS" refer to the differences of the experimental and calculated distributions with and without multiple scattering correction, respectively. The vertical bars indicate the relative contributions of different distances.

C_{2v} symmetry was assumed for the dimer, and thus the symmetry lowering of the thermal average structure is accounted for and the bond length determination is not influenced by the shrinkage.

The consequences of dynamical intramolecular interatomic scattering have been taken into account. This effect, referred to often as intramolecular multiple scattering, may be important in the electron diffraction analyses of molecules containing heavy atoms, especially if these atoms are connected at right angles, such as in Au_2F_6. As the difference curves between the experimental and calculated radial distributions show—the latter without and with dynamic scattering—this multiple scattering should not be ignored for Au_2F_6, indeed. The contribution of multiple scattering to the total experimental intensities was taken into account by using the program MUSCAT[26] that applies Glauber's theory[27] modified by the intratarget propagation model.[28] All triplet terms were included. The improved fit of the experimental and theoretical distributions can be seen in Figure 4, which displays the radial distribution curves.

The bond angles and the average and difference of the two bond lengths were independent parameters, together with the puckering angle of the thermal average structure. The geometrical parameters are given in Table 6, and the vibrational amplitudes are given in Table 5. The asymmetry parameters

Table 6. Geometrical Parameters of Au_2F_6[a]

parameter	600 K	1094 K
$r_g(Au-F)_t$[b]	1.876 ± 0.006	1.885 ± 0.011[c]
$l(Au-F)_t$	0.049 ± 0.004	0.059 ± 0.006[d]
$\kappa(Au-F)_t$	$1.0 \times 10^{-5} \pm 7.6 \times 10^{-6}$ [e]	$2.3 \times 10^{-5} \pm 2.2 \times 10^{-5}$ [f]
$r_g(Au-F)_b$[g]	2.033 ± 0.007	2.055 ± 0.014
$l(Au-F)_b$	0.067 ± 0.004	0.086 ± 0.006
$\kappa(Au-F)_b$	$2.4 \times 10^{-5} \pm 1.3 \times 10^{-5}$ [e]	$8.1 \times 10^{-5} \pm 2.2 \times 10^{-5}$ [f]
$\Delta[(Au-F)_b-(Au-F)_t]$	0.157 ± 0.002	0.169[c]
$r_g(Au_1\cdots Au_2)$	3.082 ± 0.006	3.113 ± 0.021
$l(Au_1\cdots Au_2)$	0.095 ± 0.003	0.111 ± 0.038
$\angle_a F_t-Au-F_t$	91.3 ± 1.0	91.3[h]
$\angle_\alpha F_t-Au-F_t$	92.1 ± 1.0	
$\angle_a F_b-Au-F_b$	79.9 ± 1.6	79.9[h]
$\angle_\alpha F_b-Au-F_b$	80.4 ± 1.6	
$\angle_a$[i]	17.4 ± 9.0	17.4[h]
dimer (%)	100.0	5.6 ± 4.0

[a] Bond lengths and vibrational amplitudes in angstroms, asymmetry parameter (κ) in cubic angstroms, angles in degrees. Error limits are estimated total errors, including systematic errors and the effect of constraints used in the refinement. They were obtained by the expression $\sigma_t = (2\sigma_{LS}^2 + (cp)^2 + \sum\Delta_i^2)^{1/2}$, where σ_{LS} is the standard deviation of the least-squares refinement, p is the parameter, c is 0.002 for distances and 0.02 for amplitudes, and Δ_i are the estimated effects of different constraints. See text for details. [b] Terminal Au−F bond length. [c] Difference of the two dimer and two monomer bond lengths taken from the computation at the B3LYP/Au (basis 2) and -F (aug-cc-PVTZ) level (see Table 2). [d] Refined in a group with the amplitudes of the other dimer and the two monomer Au−F bond lengths. [e] For conditions refining the two asymmetry parameters separately, see text. [f] Refined in a group with the asymmetry parameters of the other dimer and the monomer bond lengths. [g] Bridging Au−F bond length. [h] Assumed from the low-temperature experiment. [i] Puckering of the four-membered ring of the dimer.

(κ) of the two different Au−F distances could not be refined together with the bond length difference, and a series of trial calculations have been carried out with different refinement schemes and widely differing starting parameters. The effects of different constraints on the determined parameters have been carefully checked and taken into account in the error estimation.

Our electron diffraction results indicate that the dimer has a planar halogen-bridged equilibrium geometry that appears puckered in the electron diffraction analysis, as a consequence of the shrinkage effect.

Higher-Temperature Experiment. The second experiment aimed at the determination of the structure of monomeric AuF_3. With careful choice of the experimental conditions, the vapor still contained about 6% dimers in the best experiments. This is still a considerable "contamination", considering the strong scattering of the Au···Au contribution as witnessed by the radial

(26) Miller, B. R., Intramolecular Multiple Scattering Program.
(27) Glauber R. J. In *Lectures in Theoretical Physics Vol. I*; Brittin, W. E., et al., Eds.; Interscience: New York, NY, 1959.
(28) Miller, B. R.; Bartell, L. S. *J. Chem. Phys.* **1980**, *72*, 800.

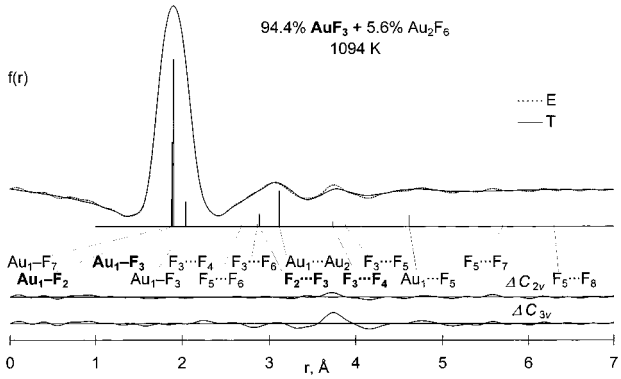

Figure 5. Experimental (E) and calculated (T) radial distributions; experiment at 1094 K. The difference curves (Δ) for the final C_{2v} model and a C_{3v} model, corresponding to a D_{3h} equilibrium structure, are indicated. The vertical bars indicate the relative contributions of different distances, with the monomer contributions in boldface.

distribution curve in Figure 5. The presence of other molecular species, such as F_2, AuF, and Au_2F_2, was also checked and could be ruled out.

Due to the complexity of the system only the conventional, so-called static analysis could be carried out, applying some assumptions. Thus, most of the nonbonded amplitudes of the dimer were taken from the normal coordinate analysis (see Table 5). The bond angles of the dimer were assumed from the results of the lower temperature experiment. Since the bond angles are related to ratios of internuclear distances, this was a reasonable assumption. There are four different Au−F bond distances in the two molecules to consider, two of the supposedly Jahn−Teller distorted monomer and two of the dimer; the assumptions concerning them were based on the computations.

Due to the different physical meaning of the computed and experimentally determined geometries—equilibrium and vibrationally averaged structures, respectively[29]—it has been a common approach to transfer *differences* of bond lengths rather than their actual values from computation to experiment.[30] The advantage of this approach is that the differences in physical meaning, as well as the effect of approximations used in the computations, would largely cancel. Our previous experience shows,[31] however, that even this assumption may be too crude, and it is prudent to check the constancy of bond length differences from computations before transferring them to the experiment as constraints. Thus, several different levels of computation and different basis sets have been tested (see Table 2). The B3LYP computations, applying basis 2 for gold and the aug-cc-PVTZ basis set for fluorine, were selected on the basis of their reasonable geometrical parameters. The difference of 0.169 Å between the two dimer bond lengths from this computation is somewhat larger than the difference at our low-temperature experiment, 0.157(2) Å. However, it was reasonable to assume that the increase in bond length at higher temperatures can be expected to be larger for the more compliant bridging bond than for the more rigid terminal bond of the dimer. The effect of using bond length differences from other computations was also tested and considered in the error estimation. The electron diffraction analysis was carried out in the so-called r_a representation, while the differences taken from the computation are differences of r_e parameters. Careful consideration of the transformation of r_a parameters to r_e showed that the correction terms largely cancel, and it is justified to use the r_e differences in the electron diffraction analysis without further change. The uncertainty of this approach was considered in the estimated total error.

Table 7. Geometrical Parameters of AuF_3[a]

parameter	r, ∠	l	κ
$r_g(Au_1-F_2)$	1.893 ± 0.012	0.063 ± 0.006 [b]	$3.3 \times 10^{-5} \pm 2.2 \times 10^{-5}$ [c]
$\Delta[(Au_1-F_3)-(Au_1-F_2)]$[d]	0.020		
$\Delta[(Au_1-F_3)-(Au-F)_t]$[d,e]	0.027		
$r_g(Au_1-F_3)$	1.913 ± 0.008	0.060 ± 0.006[b]	$2.5 \times 10^{-5} \pm 2.2 \times 10^{-5}$ [c]
$r_g(F_2\cdots F_3)$	2.950 ± 0.057	0.242 ± 0.061	
$r_g(F_3\cdots F_4)$	3.748 ± 0.029	0.105[f]	
$\angle_a F_2-Au_1-F_3$	100.1 ± 1.9		
$\angle_\alpha F_2-Au_1-F_3$	102.5 ± 1.9		
$\angle_a F_3-Au_1-F_4$	157.0 ± 4.1		
$\angle_\alpha F_3-Au_1-F_4$	160.4 ± 4.1		
monomer (%)	94.4 ± 4.0		

[a] Bond lengths and vibrational amplitudes in angstroms, asymmetry parameter (κ) in cubic angstroms, angles in degrees. Error limits are estimated total errors, including systematic errors and the effect of constraints used in the refinement, see text and Table 6 for details. For numbering of atoms see Figure 3. [b] Refined in a group with the amplitudes of the dimer Au−F bond lengths. [c] Refined in a group with the asymmetry parameters of the dimer bond lengths. [d] Difference of bond lengths taken from the computation at the B3LYP/Au (basis 2), -F (aug-cc-PVTZ) level. [e] $Au-F_t$ is the dimer terminal bond length. [f] Value taken from the normal coordinate analysis.

The following strategy was applied in treating the asymmetry parameters of the four bond distances. First we calculated the value of the Morse parameter, a, for both the dimer terminal and dimer bridging bonds from their asymmetry parameters using the expression[32,33] $a = 6\kappa l_T^{-4}(3 - 2l_0^4 l_t^{-4})^{-1}$, where κ is the asymmetry parameter, l_T is the mean-square vibrational amplitude at the temperature of the experiment, and l_0 is the mean-square vibrational amplitude at 0 K. Based on these two a values, and using the computed vibrational amplitudes for the higher temperature, the starting values of the κ parameters for the two dimer distances were calculated by the same expression. For the two different distances of the monomer we supposed that their Morse parameters are the same as that of the terminal bond of the dimer. With these assumptions and using, again, the computed parallel vibrational amplitudes for the higher temperature, the starting κ values of the two monomer distances were calculated. Finally, these four parameters were refined in one group. Considering the many assumptions in this approach and the importance of anharmonicity in these systems, other ways of estimating the initial values of the asymmetry parameters, varying in a broad interval, were also tried, with the resulting parameters staying consistently within their standard deviations. Nonetheless, even these small differences were taken into consideration in the error estimation.

The principal question in this analysis was that of the shape of the monomeric AuF_3 molecule. Both D_{3h} (i.e., C_{3v}, considering the shrinkage effect) and the Jahn−Teller-distorted C_{2v} symmetry geometries have been tested. The difference curves of experimental and calculated radial distributions show in Figure 5 that the higher symmetry structure could be ruled out and the C_{2v} symmetry ascertained, indeed. The geometrical parameters of the monomer are given in Table 7, with the vibrational amplitudes in Table 5.

(29) Hargittai, M.; Hargittai, I. *Int. J. Quantum Chem.* **1992**, *44*, 1057.
(30) Chiu, N. S.; Ewbank,; J. D.; Askari, M.; Schäfer, L. *J. Mol. Struct.* **1979**, *54*, 185.
(31) Réffy, B.; Kolonits, M.; Hargittai, M. *J. Mol. Struct.* **1998**, *445*, 139.
(32) Kuchitsu, K. *Bull. Chem. Soc. Jpn.* **1967**, *40*, 505.
(33) Hargittai, M.; Subbotina, N. Y.; Kolonits, M.; Gershikov, A. G. *J. Chem. Phys.* **1991**, *94*, 7278.

The geometrical parameters of the dimer from this experiment are given in Table 6. The many assumptions used in the analysis were taken into consideration in estimating the total errors. These errors may seem overoptimistic considering the small amount of dimers in the vapor. However, even this small amount has a relatively large contribution to the total electron scattering, especially due to its Au···Au contribution, which is the major contribution to the peak around 3 Å (see Figure 5). The effect of shrinkage is present in the determined bond angles. Test calculations, taking into account perpendicular vibrational corrections, were carried out and the bond angles are also given in the r_α representation.

Discussion

Square planar geometries for molecules of transition metals with a d^8 electronic configuration, such as Ni(II), Pd(II), Pt(II), and Au(III), are common.[34] Our quantum chemical calculations, in agreement with previous results,[1a] found the dimer of gold trifluoride to have a planar halogen-bridged structure. The electron diffraction results are in accord with this, considering that they refer to the thermal-average structure. This structure is also in line with the nearly symmetrical square-planar arrangement around gold in the crystal of AuF_3.[7] The terminal Au−F bond length is the same, 1.876(2) and 1.876(6) Å in the crystal and in the gas at 600 K, respectively, while the bridging Au−F bond in the helical chain of the crystal, 1.998(2) Å, is somewhat shorter than the bridging bond in the dimeric gas-phase molecule, 2.033(7) Å. Gold trichloride has the same structure in its crystal, consisting of planar dimeric Au_2Cl_6 units.[1a,35] On the other hand, this structure is at variance with the usual halogen-bridged geometries of metal trihalide dimers, consisting of two tetrahedra sharing a common edge (see, for example, refs 14 and 31).

We determined the dimer structure at two different temperatures, almost 500 degrees apart, and thus have an indication of the effect of temperature on its bond lengths. The terminal bond length increases by about 0.01 Å and the bridging bond lengths by about 0.02 Å upon this temperature increase. Valuable structural information can be extracted on the dimer at 1100 K even though the dimer content of the vapor is a mere 6%. This is due to the overwhelming scattering contribution of gold (see the corresponding vertical bars under the radial distributions in Figure 5, especially the one corresponding to the Au···Au distance).

The computed and experimental geometries can be compared rigorously only if vibrational corrections are applied to the thermal-average experimental geometries.[29] The experimental equilibrium bond length can be roughly estimated by applying Morse-type anharmonic corrections;[36] however, concerning the uncertainties of the asymmetry parameters in this study, we did not feel it prudent to do so. It can be estimated though, on the basis of similar systems and the temperature of the experiments, that this may amount to about 0.01−0.02 Å. From the comparison of different basis sets and computational levels, the following conclusions can be drawn: the use of basis 2 instead of basis 1 on gold causes only minor improvement in the parameters. On the other hand, the use of the Dunning triple-ζ basis on fluorine considerably improves the bond lengths compared to those obtained with the 6-311+G(3df) basis at all levels. MP2 calculations give smaller bond lengths than B3LYP with all basis sets. Thus, the MP2 level combined with the aug-cc-pVTZ basis set on fluorine somewhat underestimates the bond lengths, while both the B3LYP/aug-cc-PVTZ and the MP2/6-311+G(3df) combinations slightly overestimate them. In all the other calculations the bond lengths are too large.

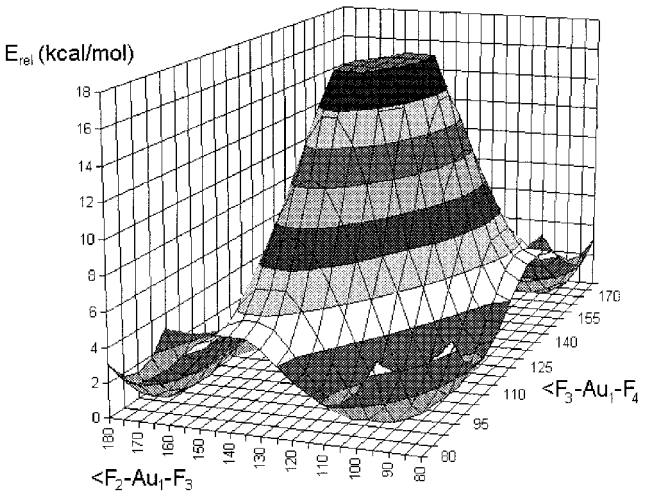

Figure 6. "Mexican-hat"-type potential energy surface for AuF_3, calculated at the B3LYP level: Au, basis 1, and F, aug-cc-pVDZ.

Bond angles are relatively insensitive to the level of the computation. The agreement between computed and experimental bond angles is acceptable for the dimer and is poorer for the monomer. Part of the disagreement may originate from the shrinkage effect. The experimental determination of the monomer bond angles suffers from the very small relative weights of the F···F contributions to the total electron diffraction intensities.

The four-member rings of the dimers of AuF_3 and AuF are rather different. The Au−F_b bridging bond length is about 0.2 Å larger in Au_2F_2 than in Au_2F_6, and further, the F−Au−F angle is more than 20° larger in Au_2F_2 than in Au_2F_6. Thus, the Au···Au distance in the monohalide dimer is very short, between 2.71 and 2.88 Å, depending on the level of the computation. This effect is often called "aurophylic"[37] and is due partly to correlation and partly to relativistic effects. Relativistic effects have a large influence on gold chemistry, larger in gold monofluoride than in gold trifluoride. While the two Au−F bond lengths shorten by about 0.05 Å in AuF_3 if relativistic effects are considered in the computation,[1a] the same shortening for AuF is about 0.16 Å.[1d] This is due to the difference in their electronic configurations. The valence shell of gold in AuF only contains the 6s orbital, and that shrinks substantially due to relativistic effects. On the other hand, in Au(III) molecules the 5d orbital becomes part of the valence shell, and their relativistic expansion partially compensates for the relativistic contraction of the 6s orbitals; thus, the overall contraction will be much smaller.

AuF_3 has a T-shaped structure as a result of a first-order Jahn−Teller symmetry breaking of the D_{3h} trigonal planar structure into the C_{2v} arrangement. Both the computations and the electron diffraction study show this distortion unambiguously. This makes AuF_3 a useful case for electron diffraction in illustrating the Jahn−Teller effect since the splitting of the F···F peak proves the distortion without a doubt. Jahn−Teller

(34) (a) Greenwood, N. N.; Earnshaw, A. *Chemistry of the Elements*; Pergamon Press: Oxford, 1984. (b) Huheey, J. E. *Inorganic Chemistry*, 3rd ed.; Harper & Row: Cambridge, MA, 1983; pp 409−410 and 470−471.

(35) Clark, E. S.; Templeton, D. H.; MacGillavry, C. H. *Acta Crystallogr.* **1958**, *11*, 284.

(36) Bartell, L. S. *J. Chem. Phys.* **1955**, *23*, 1219.

(37) (a) Schmidbaur, H. *Gold Bull.* **1990**, *23*, 11. (b) Pyykkö, P.; Runeberg, N.; Mendizabal, F. *Chem. Eur. J.* **1997**, *3*, 1451.

distortion has already been shown for AuF_3 by an earlier HF computation and has also been observed for other AuL_3 compounds (L = H, F, Cl).[1a]

The potential energy surface of AuF_3 is of a typical "Mexican-hat" type, as shown in Figure 6. It has three equivalent minima, each of C_{2v} symmetry, with a different unique F atom along the C_2 axis [E_{min1}(94.6°,170.8°); E_{min2}(170.8°,94.6°), and E_{min3}-(94.6°,94.6°)]. There are three other stationary points located on the PES, between the minima along the rim of the hat, with one imaginary frequency, and thus corresponding to three equivalent transition states. According to intrinsic reaction coordinate calculations, these transition states represent the exchange of one equatorial fluorine atom into an axial one. The barrier between the ground-state and transition-state structures is about 3−8 kcal/mol, depending on the level of the computation; it is smallest from CASSCF and largest from MP2 (see Table 3). The undistorted D_{3h} symmetry structure is in the middle of the potential energy surface with high energy and two imaginary frequencies.

Acknowledgment. This work was supported by the Hungarian Scientific Research Fund (Grant No. OTKA T 025788), the North Atlantic Treaty Organization (NATO, OUTR.LG972066), and the Fonds der Chemischen Industrie. A.S. acknowledges the Computer Center of Munich (LRZ) for grants of computer time. We are indebted to Dr. Michael Dolg for providing further information on Au pseudopotentials and basis sets. M.H. thanks Professor L. S. Bartell for his numerous suggestions and valuable advice.

Supporting Information Available: Symmetry coordinates for the ground-state geometry of AuF_3 (C_{2v}) and Au_2F_6 (D_{2h}), elements of the F-matrix for AuF_3 and Au_2F_6, total experimental intensities of gold trifluoride at two different temperatures and two different camera ranges for both (PDF). This material is available free of charge via the Internet at http://pubs.acs.org.

JA992638K